Structural Safety 69 (2017) 68–78

Contents lists available at ScienceDirect

Structural Safety

journal homepage: www.elsevier.com/locate/strusafe

Estimation and impacts of model parameter correlation for seismic performance assessment of reinforced concrete structures

B.U. Gokkaya *, J.W. Baker, G.G. Deierlein

Civil & Environmental Engineering Department and John A. Blume Earthquake Engineering Center, Stanford University, Stanford, CA 94305, United States

ARTICLE INFO

Article history:
Received 31 July 2016
Received in revised form 29 March 2017
Accepted 25 July 2017

Keywords:
Correlation
Modeling uncertainty
Random effects regression
Uncertainty propagation
Collapse

ABSTRACT

Consideration of uncertainties, including stochastic dependence among uncertain parameters, is known to be important for estimating seismic risk of structures. In this study, we characterize the dependence of modeling parameters that define a structure's nonlinear response at a component level, and the interactions of multiple components associated with a structure's response. We use random effects regression models to estimate correlations among parameters. The models are applied to a component test database with multiple tests conducted by differing research groups. Multiple tests that are conducted by a research group are subject to similar conditions and are conducted to investigate the impacts of particular properties of components. The set of tests can effectively represent components at different locations in a structure, and so are suitable for estimating stochastic dependence in model parameters. Regression models can be applied to the database to compute correlation coefficients that reflect statistical dependency among properties of components tested by individual research groups. It is assumed here that these correlation coefficients also reflect correlations associated with multiple components in a structure. To illustrate, correlations for reinforced concrete element parameters are estimated from a database of reinforced concrete beam-column tests, and then used to assess the effects of correlations on dynamic response of a frame structure. Increased correlations are seen to increase dispersion in dynamic response and produce higher estimated probabilities of collapse. This work provides guidance for characterization of parameter correlations when propagating uncertainty in seismic response assessment of structures.

1. Introduction

Performance-based earthquake engineering enables quantification and propagation of uncertainties in a probabilistic framework to make robust estimations of seismic risk and loss of structures. Quantification and propagation of ground motion uncertainties have received significant attention in the research community, but an important and somewhat less-explored topic is uncertainty in structural modeling (e.g., [12]). The uncertainties related to use of idealized models and analysis methods, as well as uncertainties in a model's parameters, influence assessments of the seismic reliability of a structure. Explicit quantification of uncertainties and characterization of dependence among the random model parameters are essential for propagating these uncertainties when assessing seismic performance.

While quantification of model parameter uncertainties is relatively well studied, stochastic dependence among model parameters has received very little attention, in large part due to scarcity of appropriate calibration data. When it has been assessed or considered in assessments, it is typically in the form of correlation coefficients. Where the random variables have a multivariate normal distribution, correlations provide a complete description of their dependence. They are also useful in first-order and other approximate reliability assessments.

The current state-of-the-art in seismic reliability analysis is to use judgment in quantifying the correlation structure of analysis model parameters. Haselton [25] used judgment-based correlation coefficients when considering model parameter uncertainty in assessing collapse risk of reinforced concrete structures, and showed that variability in collapse capacity was strongly influenced by the correlation assumptions. Liel et al. [38], Celarec and Dolsek [13], Celik and Ellingwood [14] and Pinto and Franchin [54]all used assumed correlations among modeling parameters when propagating modeling uncertainty for seismic performance assessment of reinforced concrete structures.

Although the effects of correlations among random variables on general system reliability problems are well known, few researchers have used observational data to quantify dependence. Idota

* Corresponding author.
E-mail addresses: beliz@alumni.stanford.edu (B.U. Gokkaya), bakerjw@stanford.edu (J.W. Baker), ggd@stanford.edu (G.G. Deierlein).

http://dx.doi.org/10.1016/j.strusafe.2017.07.005
0167-4730/

et al. [31] assessed the correlation of strength parameters for steel moment resisting frames using steel coupon tests from production lots. Vamvatsikos [69] used those results to study the effects of correlation of components at different locations in a building on its dynamic response. We are aware of no other studies that directly estimate correlations in component-level or phenomenological modeling parameters in order to study seismic collapse risk.

In this study, we estimate the correlation structure of modeling parameters that define a component's nonlinear cyclic response, and study the interaction of different components on system-level dynamic response. Random effects regression is used with a database of reinforced concrete column tests to infer correlation structure of parameters defining a concentrated plasticity model. The database is composed of reinforced concrete column tests performed by multiple research groups. Correlation coefficients are obtained that represent statistical dependency among parameters within a set of tests conducted by a research group. Multiple tests conducted by a research group are subject to similar conditions and are conducted to investigate the impacts of particular properties of components. Therefore, the set of tests can effectively represent conditions different locations in a structure. And the correlation coefficients can be assumed to reflect dependency among parameters corresponding to components throughout a structural system. The assessment of correlation coefficients is discussed in the subsequent sections. We then use the estimated correlations to assess the effects of correlations on dynamic response of a four-story reinforced concrete frame building, and to explore potential simplified approaches for representing parameter correlations. Although the reported correlation results are for reinforced concrete model parameters, the presented framework can be applied for other types of materials or models.

2. Probabilistic seismic performance assessment

We use the probabilistic performance-based earthquake engineering methodology to assess structural performance (e.g., [35,15]). Nonlinear structural analyses are run using a suite of ground motions to propagate uncertainties related to ground motion variability and seismic hazard. The results from structural analyses are then related to the risk of collapse and other damage states of interest.

Evaluation of structural collapse is particularly important since seismic design provisions in building codes aim to provide adequate collapse safety of structures even in extreme events. Collapse response of structures is associated with highly nonlinear component behavior, and modeling collapse requires structural analysis models that can capture large inelastic deformations with significant cyclic strength and stiffness degradation in the elements due to repeated cycles of loading. Here we use concentrated plasticity elements to capture such effects, and perform nonlinear dynamic analysis to assess structural collapse risk.

The concentrated plasticity model proposed by Ibarra et al. [29], which has been frequently used to simulate sidesway collapse in frame structures (e.g., [78,17]), is used in this study to model component response. Specific attention is given to the correlation of model parameters used to define plastic hinges in seismic resisting moment frames. Phenomenological concentrated plasticity models are well-suited for modeling collapse of structures [16]. Model parameters that define concentrated plasticity models are generally related to physical engineering parameters by empirical relationships. These relationships link component design parameters (e.g. axial load ratio, spacing of transverse reinforcement) to model parameters via equations calibrated using regression analysis. Modeling uncertainty is more pronounced for collapse response simulations than for elastic or mildly nonlinear simulations, due to both the relatively limited knowledge of parameter values (due to more limited test data) and the highly nonlinear behavior associated with collapse.

The concentrated plasticity model has a trilinear "backbone curve", shown in Fig. 1, defined by five parameters: capping plastic rotation ($\theta_{cap,pl}$), effective stiffness (secant stiffness up to 40% of the component yield moment, EI_{stf}), yield moment (M_y), capping moment (M_c), and post-capping rotation (θ_{pc}). A sixth parameter, γ, controls the rate of deterioration (under cyclic loading) of basic strength, post-capping strength, unloading stiffness, and accelerated reloading stiffness.

The uncertainty in these modeling parameters is large, as estimated by a predictive model for these parameter values that will be discussed further below. These predictive model is a function of design parameters such as the axial load ratio, shear span ratio, lateral confinement ratio, concrete strength, rebar buckling coefficient, longitudinal reinforcement ratio, ratio of transverse tie spacing to column depth, and ratio of shear at flexural yielding to shear strength [27]. Axial load ratio is a particularly important variable in predicting component model parameters such as capping and post-capping rotation capacity and cyclic energy dissipation capacity.

For a given structural design, the parameters associated with elastic and peak strengths are moderately uncertain: the $EI_{stf}/EI_g, M_y$ and M_c/M_y parameters have logarithmic standard deviations of 0.28, 0.3 and 0.1, respectively. The parameters associated with more nonlinear displacement capacities and cyclic deterioration, however, are highly uncertain: the $\theta_{pc}, \theta_{cap,pl}$ and γ parameters have logarithmic standard deviations of 0.73, 0.59 and 0.51, respectively. We note that the variability on these parameters are significantly larger than the variability associated with other physical model parameters due to the underlying behavioral effects (reinforcing bar buckling, local flange buckling, fracture) that control the degrading response. These large variations in degrading behavior at large inelastic deformations have also been reported by Fell et al. [19] for prediction of buckling and fracture in steel braces, and Kunnath et al. [36] for simulating reinforcing bar buckling and fracture.

In this study, we aim to characterize correlation of these model parameters in a structure. Parameter correlations are grouped into within-component and between-component correlations. The former refers to correlations among modeling parameters that define response of a single component, whereas the latter refers to correlations among parameters from differing components, as illustrated Fig. 2. This distinction is useful because within-component correlations can be estimated from tests of individual components,

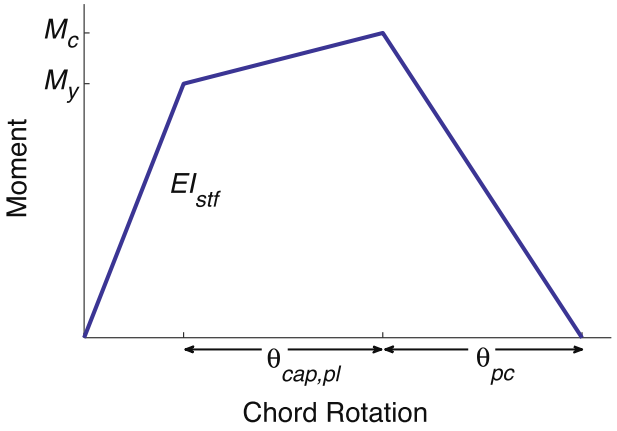

Fig. 1. Ibarra et al. [29] model for moment versus rotation of a plastic hinge in a structure. The model parameters of interest are labeled.

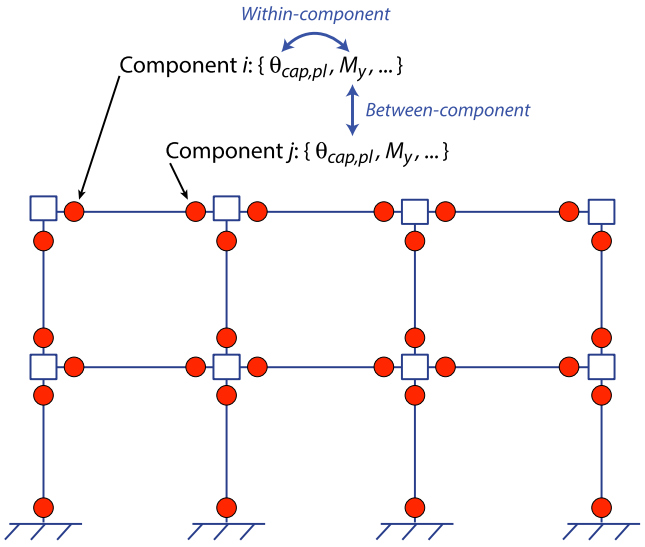

Fig. 2. Illustration of correlation within a component and correlation between components in a structure.

while between-component correlations require more effort to estimate. Between-component correlations are caused by similarities throughout a structure in the properties of structural materials, and member geometries and details. If these similarities are not captured in estimating mean values for model parameters, they will result in stochastic dependence of the resulting component model parameters.

Incremental dynamic analyses (IDA) involves performing nonlinear dynamic analysis using multiple ground motions scaled to particular ground motion intensity measure (*IM*) levels [70]. Seismic capacity is the *IM* value causing dynamic instability in the structure. This capacity is random due to the uncertain nature of a ground motion with a given *IM* level and uncertainties associated with structural performance. Its distribution is quantified by a collapse fragility function defining the probability of collapse (C) at a given *IM* level, *im* ($P(C|IM = im)$). Below, the fragility function will be estimated either by an empirical distribution or by fitting a log-normal cumulative distribution function:

$$P(C|IM = im) = \Phi\left(\frac{\ln(im/\theta)}{\beta}\right) \tag{1}$$

where $\Phi()$ is a standard normal cumulative distribution function, θ is the median and β is the logarithmic standard deviation (or "dispersion") of the distribution. Values for θ and β will be estimated and reported below.

The mean annual frequency of collapse (λ_c) is obtained by integrating a collapse fragility function with a ground motion hazard curve [28], as given in Eq. (2).

$$\lambda_c = \int_0^\infty P(C|IM = im)\left|\frac{d\lambda_{IM}(im)}{d(im)}\right| d(im) \tag{2}$$

where $\lambda_{IM}(im)$ is the mean annual rate of exceeding the ground motion *im* and $\frac{d\lambda_{IM}(im)}{d(im)}$ defines the slope of the hazard curve at *im*.

Fragility functions corresponding to alternative limit states, such as exceeding a particular story drift ratio, *sdr*, can be also obtained from incremental dynamic analysis results. Using IDA, ground motions are scaled until the structure displays a story drift ratio of *sdr* and the fragility function is obtained. This function can be integrated with the seismic hazard curve in a similar fashion to Eq. (2) to estimate the mean annual frequency ($\lambda_{SDR \geqslant sdr}$) of exceeding a given limit state.

3. Assessing correlations of model parameters

The correlation assessment procedure described in this section requires two inputs: (1) a set of observed parameter values from test data where there are groups of components analogous to a set of components in a building, and (2) predictive equations that estimate means and standard deviations of those parameters values based on component properties such as dimensions and material strengths. With those two inputs, a mixed effects analysis can be performed to estimate correlations as described here. It would also be natural to start with only the observed parameter values, and fit the predictive equations at the same time as the correlations are estimated. To illustrate, we consider the case of concrete beam-columns with the lumped-plasticity component model described above; in this case predictive equations for means and standard deviations are already available, so we adopt those equations and focus only on the estimation of correlations.

3.1. Observed parameter values

The six parameters illustrated in Fig. 1 are treated here as random variables. Haselton et al. [27] estimated values for these parameters for 255 column tests from the Pacific Earthquake Engineering Research Center Structural Performance Database [11]. This database provides force-displacement histories from cyclic and lateral-load tests, along with information related to reinforcement, column geometry, test configuration, axial load, and failure type for each column.

Haselton et al. [27] considered rectangular column tests whose failure modes were either flexure or combined flexure and shear. The model parameters were calibrated so that a cantilever column, with an elastic element and a concentrated plastic hinge at the base, has behavior that matches the corresponding experimental force-displacement data. The study authors filtered the data to remove outliers and parameters whose values could not be estimated for a given test (typically these were parameters characterizing post-peak cyclic deterioration response, in cases where a test did not induce this behavior). The total number of estimated parameter values are 232, 197, 255, 233, 65 and 223 for $\theta_{cap,pl}, EI_{stf}/EI_g, M_y, M_c/M_y, \theta_{pc}$ and γ, respectively.

The 255 column tests used for the calibration were conducted by 42 different research laboratories, referred to here as "test groups". The test groups are listed in Table 6, along with information for each regarding the variation among tests in member dimensions, concrete strength (f'_c), longitudinal yield strength (f_y), axial load ratio, and area of longitudinal and transverse reinforcement.

3.2. Evidence of parameter correlations

Using the observed parameter values described above, we compute prediction residuals by comparing the observations to model predictions:

$$\ln\left(y_{ij}^k\right) = \ln\left(\hat{y}_{ij}^k\right) + \tilde{\varepsilon}_{ij}^k \tag{3}$$

where subscripts i and j represent the test group and test number, respectively, and the superscript k indicates the random variable of interest. Random variable k from the test specified by i and j is associated with observed value y_{ij}^k, predicted value $\hat{y}_{ij}^k$, and residual $\tilde{\varepsilon}_{ij}^k$.

Predicted values are obtained in this study from the empirical equations of Haselton et al. [27] and Panagiotakos and Fardis [50]. These equations relate column design details to the six model parameters using equations that are based on regression analysis

of observed data and judgment on expected behavior. Haselton et al. [27] provide a full and a simplified equation for some of the model parameters; we use the full equations if both are provided. The predictive model studies found that parameter values are generally lognormal, so a logarithmic transformation is used in Eq. (3) (and in the original predictive models) to obtain normally distributed residuals.

For the model parameters $\theta_{cap,pl}$ and M_y, the residuals from each group of tests are plotted against each other, and a subset of the data are shown for illustration in Fig. 3. Each test group is denoted by a specific symbol and color. Grouping of these residuals by the test group implies the presence of correlated residuals; this is evident for M_y in Fig. 3b. Here it is observed that tests from group 1 (TG1) have negative residuals, implying that the M_y values of the tests conducted in that test group are consistently overestimated by the predictive equation. Conversely, tests from group 3 (TG3) have positive residuals indicating an underestimation of observations by the predictive equation.

The grouping of residuals within test groups is not surprising, considering that the tests have common features whose effects are not captured by the predictive equations. Reviewing Table 6 in the Appendix A, we observe that: 1) The majority of groups have tests with similar specimen dimensions. 2) Steel yield strength and area ratio of longitudinal reinforcing steel are constant in approximately three-quarters of the test groups. 3) The major differences among the tests within each group are the level of axial load and transverse reinforcement. While not explicitly documented, we also expect that tests from a single laboratory would have similarities in environmental conditions, workmanship, and other factors that might influence the component behavior. These features within each test group are similar to features we would expect to see among components located throughout a real-world building.

When modeling seismic performance of a real structure, we would use the same predictive equations discussed above to predict parameter values for a numerical model. Because those predictive models rely on the limited set of column properties, we would expect components in a real building to also behave in a correlated (but not perfectly dependent) manner. By assuming that a group of components in a single laboratory's tests corresponds to a group of components in a building, we can utilize statistical analysis of this test data to quantitatively estimate parameter correlations for components within a real building. While the correspondence between test groups and real-world structures is not strictly true, the authors believe it is reasonable, and this assumption provides a unique opportunity to estimate correlations that are otherwise nearly impossible to observe. We will keep in mind the approximate nature of this correspondence when evaluating the numerical results below.

3.3. Random effects regression

The observed clustering of residuals within a test group for M_y in Fig. 3b motivates studying the variability among various tests in the data. We are particularly interested in the extent to which different test groups affect the component model parameters. In this study, test groups are used as "effects" in a random effects regression model. Random effects models are linear models with at least one of the response variables having more than one categorical level [61]. The discrete levels for the categorical variable are termed the "effects" in the model, and the qualifier random implies that the observed levels represent a random sample from a population and do not contain all possible levels [62,53].

We first obtain the logarithmic residuals of each random variable, $\tilde{\varepsilon}_{ij}^k$ from Eq. (3), where subscripts i and j represent the test group and test number, respectively, and the superscript k indicates the random variable of interest. $\tilde{\varepsilon}_{ij}^k$ is then modeled using a one-way random effects regression. In this model, the test groups are treated as a random effect leading to the following equation:

$$\ln\left(y_{ij}^k\right) - \ln\left(\hat{y}_{ij}^k\right) = \tilde{\varepsilon}_{ij}^k = \mu^k + \alpha_i^k + \varepsilon_{ij}^k \tag{4}$$

where where μ^k is an intercept indicating the mean of the data for the random variable of interest. α_i^krepresents the effect of test group i on the logarithmic residual of the random variable k and $\varepsilon^k$is the residual. $\alpha_i^k$and $\varepsilon^k$are random variables with zero means and variances σ_k^2 and τ_k^2, respectively. Observations of $\alpha^k$and $\varepsilon^k$from the test

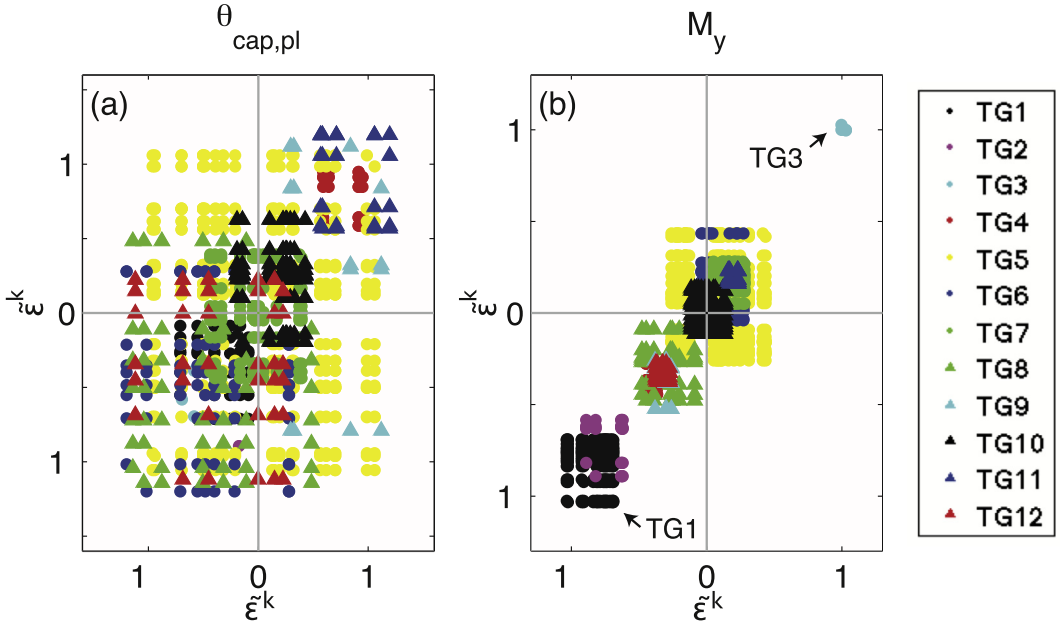

Fig. 3. Example model parameter residuals, ($\tilde{\varepsilon}^k$), plotted against the residuals of other tests within the test group to which they belong for a) $\theta_{cap,pl}$, a parameter indicating low correlation, and b) M_y, a parameter indicating higher correlation. A subset of data is shown for illustrative purposes.

data are assumed to be independent and identically distributed, and the regression procedure uses these data to estimate the variances σ_k^2 and τ_k^2. From Eq. (4) and the above definitions, $\alpha^k$and ε^krepresent between- and within-test-group variability, respectively and it follows that the variance of a model parameter, k, is $\sigma_k^2+\tau_k^2$.

After the random effects regression model given in Eq. (4) is applied to two component model parameters k and k', we can use the analysis results to study the correlation between the two variables. Following Eq. (4), the covariance of $\ln\left(y_{ij}^k\right)$ and $\ln\left(y_{ij}^{k'}\right)$ is given by:

$$\begin{aligned} cov\left(\ln\left(y_{ij}^k\right),\ln\left(y_{ij}^{k'}\right)\right) &= cov(\tilde{\varepsilon}_{ij}^k,\tilde{\varepsilon}_{ij}^{k'}) \\ &= cov(\mu^k+\alpha_i^k+\varepsilon_{ij}^k,\mu^{k'}+\alpha_i^{k'}+\varepsilon_{ij}^{k'}) \\ &= corr(\alpha_i^k,\alpha_i^{k'})\sigma_k\sigma_{k'}+corr(\varepsilon_{ij}^k,\varepsilon_{ij}^{k'})\tau_k\tau_{k'} \end{aligned} \quad (5)$$

where $cov(\cdot,\cdot)$ and $corr(\cdot,\cdot)$ refer to covariance and correlation. By definition $cov(\alpha_i^k,\alpha_j^{k'})=corr(\alpha_i^k,\alpha_i^{k'})\sigma_k\sigma_{k'}$ and $cov(\varepsilon_i^k,\varepsilon_j^{k'})=corr(\varepsilon_i^k,\varepsilon_i^{k'})\tau_k\tau_{k'}$. The values of $\alpha_i^k,\alpha_j^{k'},\varepsilon_i^k,\varepsilon_j^{k'}$ and variances are estimated from the regression procedure.

Since by definition $cov\left(\ln\left(y_{ij}^k\right),\ln\left(y_{ij}^{k'}\right)\right)=corr\left(\ln\left(y_{ij}^k\right),\ln\left(y_{ij}^{k'}\right)\right)\sigma_{\ln\left(y_{ij}^k\right)}\sigma_{\ln\left(y_{ij}^{k'}\right)}$, following Eq. (5), the correlation of $\ln\left(y_{ij}^k\right)$ and $\ln\left(y_{ij}^{k'}\right)$ is given by:

$$corr\left(\ln\left(y_{ij}^k\right),\ln\left(y_{ij}^{k'}\right)\right)=\frac{corr\left(\alpha_i^k,\alpha_i^{k'}\right)\sigma_k\sigma_{k'}+corr\left(\varepsilon_{ij}^k,\varepsilon_{ij}^{k'}\right)\tau_k\tau_{k'}}{\sqrt{\sigma_k^2+\tau_k^2}\sqrt{\sigma_{k'}^2+\tau_{k'}^2}} \quad (6)$$

Eq. (6) provides correlation of model parameters k and k' within a test group. As discussed in the preceding section, data from a particular test group are expected to have similar features to data from components in a building. Therefore, it is assumed that variability observed within test groups is indicative of the variability of different components in a structure. This assumption leads to Eq. (6) representing correlation of model parameters k and k' *within* a component j.

Using the same process, the covariance of the logarithms of the model parameters k and k' *between* components can be obtained by studying the covariance of the logarithms of the model parameters k and k' between test groups. This is given by:

$$\begin{aligned} cov\left(\ln\left(y_{ij}^k\right),\ln\left(y_{ij'}^{k'}\right)\right) &= cov(\mu^k+\alpha_i^k+\varepsilon_{ij}^k,\mu^{k'}+\alpha_i^{k'}+\varepsilon_{ij'}^{k'}) \\ &= corr(\alpha_i^k,\alpha_i^{k'})\sigma_k\sigma_{k'} \end{aligned} \quad (7)$$

where the $cov(\varepsilon_{ij}^k,\varepsilon_{ij'}^{k'})=0$ since ε_{ij}^k and $\varepsilon_{ij'}^{k'}$ are independent. Correlation of model parameters k and k' *between* components j and j' can then be shown to equal

$$corr\left(\ln\left(y_{ij}^k\right),\ln\left(y_{ij'}^{k'}\right)\right)=\frac{corr\left(\alpha_i^k,\alpha_i^{k'}\right)\sigma_k\sigma_{k'}}{\sqrt{\sigma_k^2+\tau_k^2}\sqrt{\sigma_{k'}^2+\tau_{k'}^2}} \quad (8)$$

When assessing the correlation of the same model parameter between components, $corr(\alpha_i^k,\alpha_i^k)=1$ and Eq. (8) simplifies to

$$corr\left(\ln\left(y_{ij}^k\right),\ln\left(y_{ij'}^{k}\right)\right)=\frac{\sigma_k^2}{\sigma_k^2+\tau_k^2} \quad (9)$$

We use the "lme4" package entitled (Linear Mixed-Effects Models using Eigen and S4) in the R software package [57] to perform the mixed effects regression, and then compute correlations using the above equations.

3.4. Regression results

Estimated between-component (σ_k) and within-component (τ_k) standard deviations for the example database are shown in Table 1. Table 2 shows the correlation coefficients obtained using Eqs. (5)–(9). Table 3 shows the same correlation coefficients obtained after rounding to one significant figure, reflecting the approximate nature of the way in which we are using these data and the finite sized database used here. The correlations shown in Table 3 are used in the rest of the paper.

We note that rounding of the correlation coefficients, and estimation of correlations from data with missing values, can result in a correlation matrix without the required positive semi-definiteness property. Although Table 3 produces positive definite matrices, in our initial calculations some violation of positive semi-definiteness was observed. In such cases, minor changes can be made to transform the correlation matrix into a positive definite one [32].

We observe that within a component (i.e., the left half of Table 3), correlations of model parameters are rather small; the largest coefficient being 0.3, which corresponds to the correlations between M_c/M_y and M_y, and M_c/M_y and $\theta_{cap,pl}$. These values suggest moderate interactions between strength parameters and hardening behavior. A correlation coefficient of 0.2 is obtained for the parameters defining post-capping cyclic behavior within a component (e.g., γ with M_c/M_y and θ_{pc}). The correlation of post-capping and capping plastic rotation is also obtained as 0.2 within a component.

Between components, like parameters have larger correlation coefficients (i.e., the diagonal components on the right half of Table 3). We see that $M_y,\theta_{cap,pl},EI_{stf}/EI_g$ and M_c/M_y have correlations of 0.7 or greater. In the setting of a structure, this implies that values of these parameters across components will tend to take similar values; note that Haselton and Deier [26] and Liel et al. [38]assumed perfect correlation between like parameters across components.

We also observe that correlations of different model parameters between components are small (i.e., the off-diagonal terms in the right half of the table). This is expected, given that the correlations of these parameters within a component are also small. The largest correlation among different model parameters between components is obtained as 0.2 between M_y and M_c/M_y. There is even a small negative correlation between EI_{stf}/EI_g and M_c/M_y. This is a numerical artifact from estimation using finite samples of data, as there is no clear physical reason why such a correlation would be negative.

The correlation of M_c/M_y and θ_{pc} both within a component and between components is small and these values can be approximated as 0. Specifically, the correlation between M_c/M_y and θ_{pc} within a component is observed to be 0.0077 whereas among components it is 0.0415. These values are also numerical artifacts due to the uncertainty in statistical estimates using small sample sizes.

These artifacts motivate the decision to retain only one significant figure in the correlation estimates.

Table 1
Between and within test group standard deviations obtained from random effects regression.

	σ_k	τ_k	$\sqrt{\sigma_k^2+\tau_k^2}$
$\theta_{cap,pl}$	0.41	0.44	0.59
$\frac{EI_{stf}}{EI_g}$	0.20	0.20	0.28
M_y	0.26	0.10	0.30
$\frac{M_c}{M_y}$	0.07	0.08	0.10
θ_{pc}	0.24	0.69	0.73
γ	0.20	0.46	0.51

Table 2
Initial correlation coefficients obtained from random effects regression.

		Component i						Component j					
		θ_{cap,pl_i}	$\left(\frac{EI_{stf}}{EI_g}\right)_i$	M_{y_i}	$\left(\frac{M_c}{M_y}\right)_i$	θ_{pc_i}	γ_i	θ_{cap,pl_j}	$\left(\frac{EI_{stf}}{EI_g}\right)_j$	M_{y_j}	$\left(\frac{M_c}{M_y}\right)_j$	θ_{pc_j}	γ_j
Component i	θ_{cap,pl_i}	1.0000	-0.0183	0.0578	0.2538	0.2083	-0.0260	0.6839	0.0106	0.0277	0.0975	0.0533	-0.0202
	$\left(\frac{EI_{stf}}{EI_g}\right)_i$		1.0000	0.1354	-0.1018	0.0375	0.0799		0.6853	0.0612	-0.0950	-0.0305	0.0379
	M_{y_i}			1.0000	0.2838	0.1067	0.0722			0.9263	0.2482	0.0951	0.0549
	$\left(\frac{M_c}{M_y}\right)_j$				1.0000	0.0077	0.1681				0.6728	0.0415	0.0192
	θ_{pc_i}		(sym.)			1.0000	0.2195		(sym.)			0.3466	0.0357
	γ_i						1.000						0.4102

Table 3
Final correlation coefficients are obtained after rounding to one significant figure.

		Component i						Component j					
		θ_{cap,pl_i}	$\left(\frac{EI_{stf}}{EI_g}\right)_i$	M_{y_i}	$\left(\frac{M_c}{M_y}\right)_i$	θ_{pc_i}	γ_i	θ_{cap,pl_j}	$\left(\frac{EI_{stf}}{EI_g}\right)_j$	M_{y_j}	$\left(\frac{M_c}{M_y}\right)_j$	θ_{pc_j}	γ_j
Component i	θ_{cap,pl_i}	1.0	0.0	0.1	0.3	0.2	0.0	0.7	0.0	0.0	0.1	0.1	0.0
	$\left(\frac{EI_{stf}}{EI_g}\right)_i$		1.0	0.1	-0.1	0.0	0.1		0.7	0.1	-0.1	0.0	0.0
	M_{y_i}			1.0	0.3	0.1	0.1			0.9	0.2	0.1	0.1
	$\left(\frac{M_c}{M_y}\right)_j$				1.0	0.0	0.2				0.7	0.0	0.0
	θ_{pc_i}		(sym.)			1.0	0.2		(sym.)			0.3	0.0
	γ_i						1.0						0.4

4. Impacts of parameter correlations on probabilistic estimation of dynamic response of structures

4.1. Case study structure

A reinforced concrete special moment frame structure is considered here, to demonstrate the impact of parameter correlations and evaluate potential model simplifications for structures with many uncertain parameters. The building was designed by Haselton [25] for a high seismicity site in California in accordance with 2003 IBC and ASCE 7-02 provisions [30,1]. The structural system of the ductile reinforced concrete frame building is modeled using the concentrated plasticity approach described above, in which elements of the frame are modeled using elastic elements with rotational springs at the ends. Gokkaya et al. [23] uses the correlation structure derived for lumped-plasticity models to study incorporating the uncertainty in structural model parameters in nonlinear dynamic analyses to probabilistically assess story drifts and collapse risk of buildings. An extensive set of ductile and non-ductile reinforced concrete building archetypes are used to quantify the influence of modeling uncertainties and how it is affected by the ductility and collapse modes of the structures.

Here we assume the building to be located at the same Los Angeles site as considered in its original design. One three-bay four-story frame of the building is modeled, with a total of 12 beam and 16 column elements. A Rayleigh damping of 3% is defined at the first and third mode periods of the structure, and P-Δ effects are modeled using a leaning column. The fundamental period of the structure is 0.94 s. The Open System for Earthquake Engineering Simulation platform is used to analyze the structure [49]. The FEMA-P695 far-field set of 44 ground motion components is used for structural response simulations [20].

Monte Carlo simulation is used for propagating uncertainties related to modeling and ground motion variability [33]. The six parameters mentioned previously are treated as random, with marginal means and standard deviations as predicted by Haselton et al. [27], and correlations as defined below. Further, equivalent viscous damping and column footing rotational stiffness are assumed to be random, with logarithmic standard deviation values of 0.6 and 0.3, respectively [25,24,55], and to be independent of the other parameters. A multivariate normal distribution is assumed for the logarithms of all parameters except M_c/M_y. Since, by definition M_c/M_y is always greater than 1, we use a one-sided truncated normal distribution for this parameter. Because only one frame of the structure is modeled, it is implicitly assumed that the parameters for frames in a given direction are fully correlated.

Table 4 lists four correlation models considered in the following analyses. As the name implies, the *No Correlation* model assumes all parameters in the building to be uncorrelated. This model has 170 random variables (six parameters for each of 28 elements, plus damping and foundation stiffness parameters). The *Partial Correlation A* model uses correlation coefficients from Table 3 for all within- and between-component correlations, and also has 170 random variables. In *Partial Correlation B*, Table 3 is used to define correlations within a component and correlations of beam-to-column components. Column-to-column and beam-to-beam parameters are assumed to be fully correlated (e.g., all column components for a given model realization have the same parameters). These assumed full correlations reduce the effective number of random variables for this model to 14 (six beam parameters, six column parameters, damping and foundation stiffness). In the *Full Correlation* model all of the element parameters are assumed to have perfect correlation, such that there are effectively three random variables (one component parameter, damping and foundation stiffness).

Table 4
Correlation models used with Monte Carlo simulations. "0", "P" and "1" refer to the cases of No Correlation, Partial Correlation and Perfect Correlation, respectively.

Model Name	Within component	Between-component			Effective of # R.V.s
		Column-to-Column	Beam-to-Beam	Beam-to-Column	
No Correlation	0	0	0	0	170
Partial Correlation A	P	P	P	P	170
Partial Correlation B	P	1	1	P	16
Full Correlation	1	1	1	1	3

For each correlation model, we simulate 4400 realizations of model parameters from their joint distribution, each of which are randomly matched with one ground motion. Incremental dynamic analysis is then conducted to scale each ground motion up until structural collapse is observed for the given model realization. A maximum story drift ratio (SDR) $\geqslant 0.1$ is assumed to indicate structural collapse. Ground motion *IM* values are defined as 5%-damped first-mode spectral acceleration, $Sa(0.94s)$.

4.2. Results

Fig. 4a and b show the median IDA curves from the four correlation models, along with results for a structure with median model parameters (i.e., no parameter uncertainty). There are remarkably small differences among the median IDA curves. A small difference between the *No Correlation* and *Full Correlation* cases is observed for $SDR \geqslant 0.03$, with a difference of 7% at $SDR = 0.1$. The parameters characterizing the capping and post capping behavior of components have higher uncertainty and as SDR gets higher, these parameters become more effective in characterizing the structural response. Therefore the impacts of uncertainties become more prominent as structural response becomes nonlinear and is dominated by the parameters having higher uncertainty.

Fig. 4c and d show the dispersions in the IDA curves. As can be observed from these figures, the dispersion in IDA curves increases as the level of correlation increases in the structure. The *Partial Correlation A* and *No Correlation* models yield similar variability for $SDR < 0.03$, and at $SDR = 0.1$, the difference in dispersion values for these two cases is 12%. At SDR = 0.1, the difference in dispersion between *No Correlation* and *Full Correlation* models is 47%. The *Median* model consistently underestimates dispersion, where for $SDR = 0.1$, a difference of 17% is observed between dispersion values of *Median* and *Partial Correlation* models. The *Partial Correlation A* and *B* models have very similar medians and dispersions.

Using a First-Order Second-Moment (FOSM) approach [42,7] one can show that the correlation in model parameters increases the dispersion in the estimated structural capacity. Therefore, the trends observed in Fig. 4c and d can also be explained using a first order approximation to the Taylor series expansion of structural

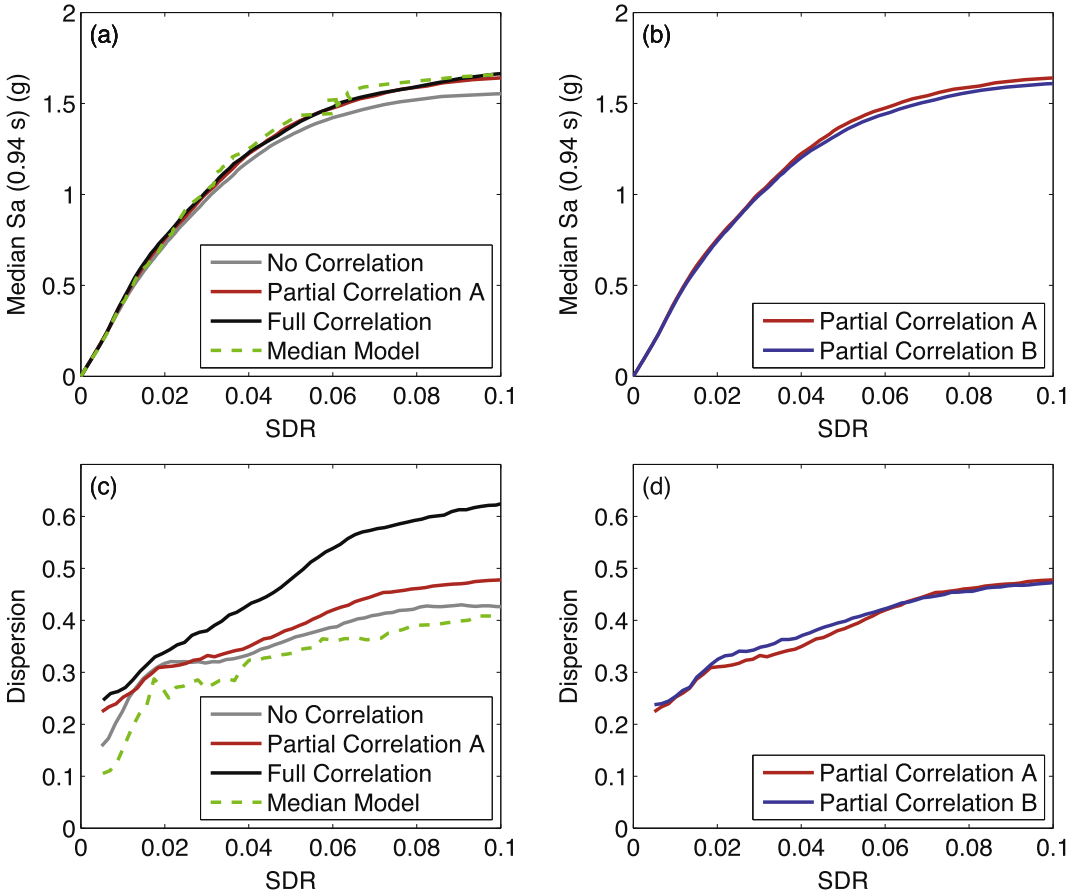

Fig. 4. IDA results obtained using different correlation models a) median IDA response for varying correlation levels, b) median IDA response for *Partial Correlation* models, c) dispersion in IDA curves for varying correlation levels, and d) dispersion in IDA curves for *Partial Correlation* models.

response. However, seismic response and its associated limit state function is mildly to strongly non-linear [71]. This makes the first-order approximation to the limit state function defining collapse response less accurate. Also, as the number of random variables grows, the computational demand of FOSM grows linearly. Therefore, in this study we use Monte Carlo simulations for the following reasons: 1) they can adapt well to the nonlinearity in limit state functions; and 2) the number of simulations are not affected by the number of random variables and thus they scale well for high-dimensional problems.

The mean annual frequency of collapse, λ_c, is obtained by integrating the empirical collapse fragility curves with the seismic hazard curve of the Los Angeles site using Eq. (2). Fragility functions and corresponding and $\lambda_{SDR\geqslant sdr}$ values are also obtained for alternative values of *sdr*. Fig. 5 shows $\lambda_{SDR\geqslant sdr}$ with respect to *sdr* using the assumed correlation models, where the $\lambda_{SDR\geqslant sdr}$ differ for *SDR* values greater than approximately 0.03. As mentioned previously, this was expected since the structural response becomes nonlinear as *SDR* grows and it is more strongly influenced by uncertainties in model parameters.

The plots show, for example, that the *No Correlation* and *Partial Correlation* cases produce nearly identical $\lambda_{SDR\geqslant sdr}$. On the other hand, the $\lambda_{SDR\geqslant sdr}$ for the *Full Correlation* case is 30% to 110% higher than the *No Correlation* model for drift values of 0.05 and 0.1, respectively. This highlights the need for reliable characterization of correlation structure in predicting structural response at near-collapse and collapse states.

Fig. 6 shows empirical collapse cumulative distribution functions for the structure obtained using the considered correlation models. At smaller $Sa(0.94\,s)$ levels, as the correlations among parameters increase, the structure has a higher probability of collapse. As expected, the median model provides smaller probabilities of collapse, especially for smaller ground motion intensities, leading to unconservative estimates of collapse risk. Note that since median collapse capacity is higher for the median model, it would result in slightly larger collapse margin ratio (i.e., the ratio of the median collapse capacity to Maximum Considered Event (MCE) intensity) [20], which can be misleading from a collapse safety point of view. The No Correlation and Partial Correlation models have similar lower tail behavior and only differ at higher *IM* levels.

Table 5 summarizes the counted median and logarithmic standard deviation (β) of collapse capacities obtained using alternative correlation models, along with the associated collapse rates. Any differences observed at the lower tail of the fragility curve due to increasing levels of correlation translate into pronounced differences in λ_c estimates. For example, there is a factor of 2.4 difference between λ_c estimates obtained using the No Correlation and Full Correlation models. The similarity in lower tail collapse fragilities for No Correlation and Partial Correlation models leads to similar

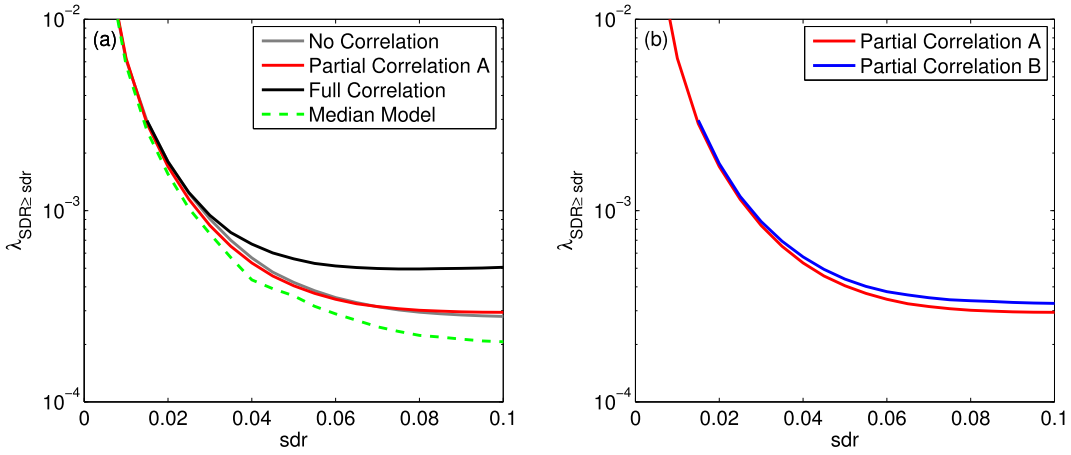

Fig. 5. Mean annual frequency of exceedance of maximum story drift ratio using the considered correlation models.

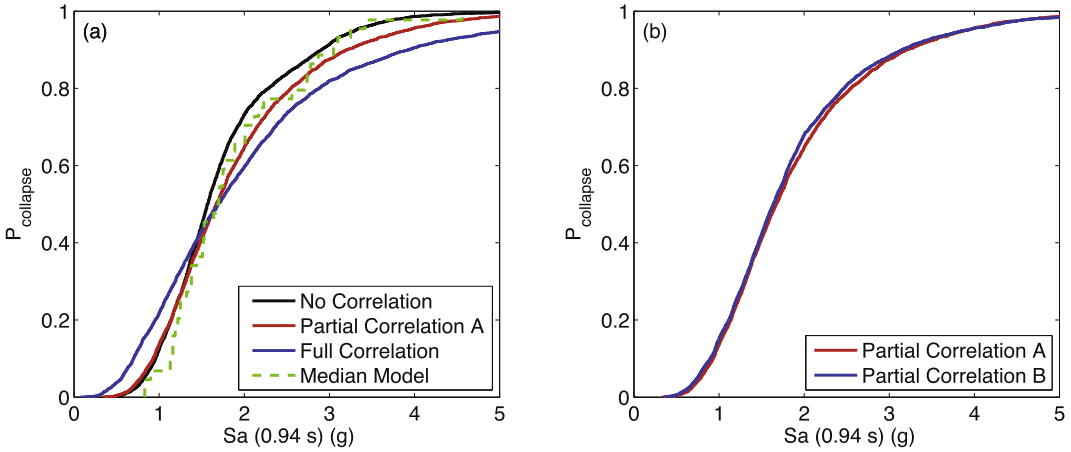

Fig. 6. Empirical cumulative distribution functions obtained using different correlation models.

Table 5
Counted median and logarithmic standard deviation (σ_{ln}) of collapse capacity, and mean annual frequency of collapse (λ_c), obtained using alternative models.

Model Name	Median	β	$\lambda_c(*10^{-4})$
Median Model	1.69	0.39	1.81
No Correlation	1.57	0.42	2.65
Partial Correlation A	1.67	0.48	2.75
Partial Correlation B	1.64	0.49	3.06
Full Correlation	1.69	0.67	6.39

λ_c estimates using these models, since the lower tail of the collapse fragility function contributes the most to λ_c [17].

Given the above results, we can make a few observations about the impact of these models, taking the *Partial Correlation A* case as a benchmark because it fully utilizes the previously estimated parameter correlations. The *Partial Correlation B* model is appealing, as it produces comparable results to the *Partial Correlation A* case, but reduces the number of modeled random variables; this is helpful when using reliability assessment procedures that scale in effort with the number of random variables. The *Full Correlation* case further reduces the number of random variables, but with an apparent loss in accuracy for this case. The Median Model and No Correlations cases are also simplified representations of the model, but they produce unconservative estimates of seismic collapse risk and so should be used with caution.

The structure considered here was designed to have a regular strength and stiffness distribution over its height, and so the typical collapse mechanisms were not notably altered when considering *No Correlation* and *Partial Correlation* models. Although we did not investigate the influence of ductility and strength irregularities in detail, we expect that different results are likely to be obtained for buildings with strength irregularities, since presence of even partial correlations may enable the triggering of alternate modes of failure (e.g., creation of a story mechanism by simulation of weak column-strength parameters).

5. Conclusions

We have considered model parameter uncertainty in seismic performance assessment of structures, both in estimating parameter correlations and in quantifying the impacts of these correlations on building performance. We have characterized the dependence of modeling parameters that define cyclic inelastic response at a component level and the interactions of multiple components associated with a system's response. Parameter correlations were estimated from component tests using random effects regression on grouped tests of structural components. Variation in parameter values within and between test groups were incorporated as random effects in the regression model, and statistical dependency between the estimated parameters were assessed.

Dependence in the parameters defining a lumped-plasticity model for concrete columns were estimated using a database of reinforced concrete beam-column tests. Correlation coefficients from these regression models, reflecting statistical dependency among properties of components tested by individual research groups, are assumed to reflect correlations among components within a given structure. The random treatment of research groups, combined with the aforementioned observations in the data set (i.e., similarity of column dimensions and differences in axial load and transverse reinforcement in the tests), justified this assumption. We found that correlations between differing parameters (both within and between components) have low correlation (correlation coefficients from −0.1 to 0.3), while like parameters across components have higher correlations of as large as 0.9.

The impact of these estimated parameter correlations on dynamic response of a four story reinforced concrete frame structure was then assessed, by performing Incremental Dynamic Analysis of the structure using Monte Carlo realizations of uncertain model parameters. Variations in correlation assumptions did not strongly influence median response, even for large drifts. Variability in correlation assumptions did, however significantly influence dispersion in response estimates, especially at large drift levels associated with severe nonlinearity and collapse. Models considering uncorrelated and partially correlated parameters had similar collapse fragility functions at the critical lower tail, resulting in similar mean annual frequencies of collapse. Models assuming perfectly correlated parameters, however, had higher probabilities of collapse for low-intensity shaking; the perfectly correlated model had a mean annual frequency of collapse that was 2.4 times the frequency of collapse of the fully uncorrelated model (even though the parameters had the same marginal distributions in both cases). A slightly simplified model representation, with full correlation among beam-to-beam and column-to-column parameters (and partially correlated beam-to-column parameters), produced nearly identical results to the benchmark model with partial correlations in all parameters. This simplified model has significantly fewer unique random variables, and so is a promising approach for considering parameter correlations while also managing computational expense. In aggregate, these results provide further evidence that parameter correlations are an important consideration in seismic collapse safety assessments.

The results presented here were for reinforced concrete components, but the framework allows these evaluations to be performed on any model with uncertain parameters that are estimated from experimental data. The correlation estimation approach requires a set of component tests with multiple tests that can be grouped and considered as having commonalities consistent with those among components in a given structure. Tests that are conducted in similar conditions, and are investigating the impacts of particular properties of components, are most suitable for this approach. While the appropriateness of considering groups of tests to represent components throughout a structure will need to be evaluated on a case-by-case basis, this proposed approach offers a unique solution to the otherwise vexing problem of estimating parameter correlations for studying the seismic reliability of buildings.

6. Data and resources

The data for the reinforced concrete column tests are obtained from the PEER Structural Performance Database (http://nisee.berkeley.edu/spd/) and Professor Curt Haselton's Reinforced Concrete Element Calibration Database (http://www.csuchico.edu/structural/researchdatabases/reinforced_concrete_element_calibration_database.shtml).

Acknowledgements

We thank Dr. Shrey Shahi and Professor Art Owen for providing valuable feedback on mixed effects modeling. We also thank two anonymous reviewers for their constructive comments. This work was supported by the National Science Foundation under NSF Grant No. CMMI-1031722. Any opinions, findings and conclusions or recommendations expressed in this material are those of the authors and do not necessarily reflect the views of the National Science Foundation.

Appendix A. Information on test groups conducting reinforced concrete column tests

This appendix provides summary data of the test groups of concrete component tests considered here. The variables in the table

Table 6
Test groups conducting reinforced concrete column tests. "Y" and "–" indicate when the tests within the test group have similar or different properties, respectively. "N/A" is used when the group has only one test.

Test Group	Reference	# Tests	Dim.	f'_c	f_y	Are the properties similar among tests? *ALR*	*LRS*	*TRS*
1	Galeota et al. [21]	24	Y	Y	Y	–	–	–
2	Bayrak and Sheikh [9]	16	–	–	–	–	–	–
3	Pujol [56]	14	Y	–	Y	–	Y	–
4	Wight and Sozen [74]	13	Y	–	Y	–	Y	–
5	Matamoros [41]	12	Y	–	–	–	–	–
6	Thomson and Wallace [68]	11	Y	–	–	–	Y	–
7	Atalay and Penzien [5]	10	Y	–	–	–	Y	–
8	Saatcioglu and Grira [58]	10	Y	Y	–	–	–	–
9	Mo and Wang [43]	9	Y	–	Y	–	Y	–
10	Bayrak and Sheikh [8]	8	Y	–	Y	–	Y	–
11	Muguruma et al. [44]	8	Y	–	Y	–	Y	Y
12	Tanaka [67]	8	–	–	–	–	–	–
13	Sakai [60]	7	Y	Y	–	Y	–	–
14	Kanda et al. [34]	6	Y	–	Y	–	Y	Y
15	Legeron and Paultre [37]	6	Y	–	–	–	Y	–
16	Paultre et al. [52]	6	Y	–	Y	–	Y	–
17	Saatcioglu and Ozcebe [59]	6	Y	–	–	–	Y	–
18	Takemura and Kawashima [66]	6	Y	–	Y	Y	Y	Y
19	Xiao and Yun [76]	6	Y	–	Y	–	Y	–
20	Xiao and Martirossyan [75]	6	Y	–	Y	–	–	–
21	Zhou et al. [80]	6	Y	–	Y	–	Y	–
22	Bechtoula [10]	5	–	–	–	–	–	–
23	Sugano [65]	5	Y	Y	Y	–	Y	–
24	Watson [72]	5	Y	–	Y	–	Y	–
25	Esaki [18]	4	Y	–	Y	–	Y	–
26	Gill [22]	4	Y	–	Y	–	Y	–
27	Soesianawati [64]	4	Y	–	Y	–	Y	–
28	Wehbe et al. [73]	4	Y	–	Y	–	Y	–
29	Ohno and Nishioka [46]	3	Y	Y	Y	Y	Y	Y
30	Sezen and Moehle [63]	3	Y	–	Y	–	Y	Y
31	Ang [3]	2	Y	–	Y	–	Y	–
32	Azizinamini et al. [6]	2	Y	–	Y	–	Y	–
33	Lynn et al. [40]	2	Y	–	Y	–	–	–
34	Lynn [39]	2	Y	–	Y	–	Y	Y
35	Ohue et al. [47]	2	Y	–	–	–	–	Y
36	Ono et al. [48]	2	Y	Y	Y	–	Y	Y
37	Zahn [77]	2	Y	–	Y	–	Y	–
38	Zhou et al. [79]	2	Y	–	Y	–	Y	Y
39	Amitsu et al. [2]	1	N/A	N/A	N/A	N/A	N/A	N/A
40	Arakawa et al. [4]	1	N/A	N/A	N/A	N/A	N/A	N/A
41	Nagasaka [45]	1	N/A	N/A	N/A	N/A	N/A	N/A
42	Park and Paulay [51]	1	N/A	N/A	N/A	N/A	N/A	N/A

are defined as follows: "Dim." is member dimensions, f'_c is concrete compressive strength, f_y is reinforcing steel yield strength, *ALR* is Axial Load Ratio, *LRS* is the ratio of Longitudinal Reinforcing Steel to section area, *TRS* is the ratio of Transverse Reinforcing Steel to section area.

References

[1] American Society of Civil Engineers. ASCE standard 7-02: minimum design loads for buildings and other structures. VA: Reston; 2002.
[2] Amitsu S, Shirai N, Adachi H, Ono A. Deformation of reinforced concrete column with high or fluctuating axial force. Trans Jpn Concr Inst 1991;13:35–362.
[3] Ang BG. Ductility of reinforced concrete bridge piers under seismic loading [Master's thesis]. University of Canterbury. Civil and Natural Resources Engineering; 1981.
[4] Arakawa T, Arai Y, Egashira K, Fujita Y. Effects of the rate of cyclic loading on the load-carrying capacity and inelastic behavior of reinforced concrete columns. Trans Jpn Concr Inst 1982;4:485–92.
[5] Atalay MB, Penzien J, Behavior of critical regions of reinforced concrete components as influenced by moment, shear and axial force. Earthquake Engineering Research Center, Report No. EERC 75, 19; 1975.
[6] Azizinamini A, Johal LS, Hanson NW, Musser DW, Corley WG. Effects of transverse reinforcement on seismic performance of columns: A partial parametric investigation Technical report. Construction Technology Laboratories Inc.; 1988.
[7] Baker JW, Cornell CA. Uncertainty specification and propagation for loss estimation using FOSM methods Technical Report 2003/07. Berkeley, California: Pacific Earthquake Engineering Research Center, University of California at Berkeley; 2003.
[8] Bayrak O, Sheikh SA. Confinement steel requirements for high strength concrete columns. In: Proceedings of the 11th world conference on earthquake engineering, number 463. Elsevier Science Ltd.; 1996.
[9] Bayrak O, Sheikh SA. Plastic hinge analysis. J Struct Eng 2001;127 (9):1092–100.
[10] Bechtoula H. Damage assessment of reinforced concrete columns under large axial and lateral loadings Technical report. Dept. of Architecture and Architectural Systems, Kyoto University; 1985.
[11] Berry M, Parrish M, Eberhard M. PEER structural performance database users manual (version 1.0). Berkeley: University of California; 2004.
[12] Bradley BA. A critical examination of seismic response uncertainty analysis in earthquake engineering. Earthquake Eng Struct Dyn 2013;42 (11):1717–29.
[13] Celarec D, Dolsek M. The impact of modelling uncertainties on the seismic performance assessment of reinforced concrete frame buildings. Eng Struct 2013;52:340–54.
[14] Celik OC, Ellingwood BR. Seismic fragilities for non-ductile reinforced concrete frames Role of aleatoric and epistemic uncertainties. Struct Saf 2010;32 (1):1–12.
[15] Deierlein GG. Overview of a comprehensive framework for earthquake performance assessment. Technical report, International Workshop on Performance-Based Seismic Design Concepts and Implementation, Bled, Slovenia; 2004.
[16] Deierlein GG, Reinhorn AM, Willford MR. Nonlinear structural analysis for seismic design. NEHRP Seismic Design Technical Brief (NIST GCR 10-917-5), 4; 2010.

[17] Eads L, Miranda E, Krawinkler H, Lignos DG. An efficient method for estimating the collapse risk of structures in seismic regions. Earthquake Eng Struct Dyn 2013;42(1):25–41.
[18] Esaki F. Reinforcing effect of steel plate hoops on ductility of r/c square columns. In: Proc., 11th world conf. on earthquake engineering. Pergamon: Elsevier Science; 1996. p. 199.
[19] Fell BV, Kanvinde AM, Deierlein GG, Myers AT, Fu X. Buckling and fracture of concentric braces under inelastic cyclic loading. Technical Report Steel Tips 94. Structural Steel Education Council; 2006.
[20] FEMA. Quantification of building seismic performance factors. FEMA-P695. Federal Emergency Management Agency; 2009.
[21] Galeota D, Giammatteo MM, Marino R. Seismic resistance of high strength concrete columns. In: Proceedings of the 11th world conference on earthquake engineering, number 1383. Elsevier Science Ltd; 1996.
[22] Gill WD. Ductility of rectangular reinforced concrete columns with axial load. Technical report. New Zealand: University of Canterbury, Department of Civil Engineering; 1979.
[23] Gokkaya BU, Baker JW, Deierlein GG. Quantifying the impacts of modeling uncertainties on the seismic drift demands and collapse risk of buildings with implications on seismic design checks. Earthquake Eng Struct Dyn 2016;45(10):1661–83.
[24] Hart GC, Vasudevan R. Earthquake design of buildings:damping. J Struct Div 1975;101(1):11–30.
[25] Haselton C. Assessing seismic collapse safety of modern reinforced concrete moment frame buildings. Stanford, CA: Dept. of Civil and Environmental Engineering. Stanford University; 2006.
[26] Haselton CB, Deierlein GG. Assessing seismic collapse safety of modern reinforced concrete moment frame buildings. Technical report, Report 2007/08. Berkeley, CA: Pacific Earthquake Engineering Research Center; 2007.
[27] Haselton CB, Liel AB, Lange ST, Deierlein GG. Beam-column element model calibrated for predicting flexural response leading to global collapse of RC frame buildings. Technical Report PEER 2007/03. Berkeley, California: Pacific Earthquake Engineering Research Center, University of California at Berkeley; 2008.
[28] Haselton CB, Liel AB, Lange ST, Deierlein GG. Beam-column element model calibrated for predicting flexural response leading to global collapse of RC frame buildings. Technical Report PEER 2007/03. Berkeley, California: Pacific Earthquake Engineering Research Center, University of California at Berkeley; 2008.
[29] Ibarra LF, Medina RA, Krawinkler H. Hysteretic models that incorporate strength and stiffness deterioration. Earthquake Eng Struct Dyn 2005;34(12):1489–511.
[30] IBC. International Building Code. International Code Council. ISBN: 1892395568; 2003.
[31] Dota H, Guan L, Yamazaki K. Statistical correlation of steel members for system reliability analysis. In: Proceedings of the 9th international conference on structural safety and reliability (ICOSSAR), Osaka, Japan.
[32] Jackel P. Monte Carlo methods in finance. Stochastic Dyn 2001;3. 3–2.
[33] Kalos MH, Whitlock PA. Monte Carlo methods. John Wiley & Sons; 2009.
[34] Kanda M, Shirai N, Adachi H, Sato T. Analytical study on elasto-plastic hysteretic behaviors of reinforced concrete members. Trans Jpn Concr Inst 1988;10:257–64.
[35] Krawinkler H, Miranda E. Performance-based earthquake engineering. In: Bozorgnia Y, Bertero VV, Bertero, editors. Earthquake engineering: from engineering seismology to performance-based engineering. Boca Raton, USA: CRC Press; 2004.
[36] Kunnath SK, Heo Y, Mohle JF. Nonlinear uniaxial material model for reinforcing steel bars. J Struct Eng 2009;135(4):335–43.
[37] Legeron F, Paultre P. Behavior of high-strength concrete columns under cyclic flexure and constant axial load. ACI Struct J 2000;97(4).
[38] Liel AB, Haselton CB, Deierlein GG, Baker JW. Incorporating modeling uncertainties in the assessment of seismic collapse risk of buildings. Struct Saf 2009;31(2):197–211.
[39] Lynn AC. Seismic evaluation of existing reinforced concrete building columns [Ph.D. thesis]. University of California at Berkeley; 2001.
[40] Lynn AC, Moehle JP, Mahin SA, Holmes WT. Seismic evaluation of existing reinforced concrete building columns. Earthquake Spectra 1996;12(4):715–39.
[41] Matamoros AB. Study of drift limits for high-strength concrete columns [Ph.D. thesis]. University of Illinois at Urbana-Champaign; 1999.
[42] Melchers RE. Structural reliability analysis and prediction, vol. 2. New York: John Wiley, Chichester; 1999.
[43] Mo Y-L, Wang S. Seismic behavior of rc columns with various tie configurations. J Struct Eng 2000;126(10):1122–30.
[44] Muguruma H, Watanabe F, Komuro T. Applicability of high strength concrete to reinforced concrete ductile column. Trans Jpn Concr Inst 1989;11(1):309–16.
[45] Nagasaka T. Effectiveness of steel fiber as web reinforcement in reinforced concrete columns. Trans Jpn Concr Inst 1982;4:493–500.
[46] Ohno T, Nishioka T. An experimental study on energy absorption capacity of columns in reinforced concrete structures. Proc JSCE Struct Eng/Earthquake Eng 1984;1(2):137–47.
[47] Ohue M, Morimoto H, Fujii S. Behavior of rc short columns failing in splitting bond-shear under dynamic lateral loading. Trans Jpn Concr Inst 1985;7:293–300.
[48] Ono A, Shirai N, Adachi H, Sakamaki Y. Elasto-plastic behavior of reinforced concrete column with fluctuating axial force. Trans Jpn Concr Inst 1989;11:239–46.
[49] OpenSEES. pen system for earthquake engineering simulation.http://opensees.berkeley.edu/; 2015 [accessed: 08.28.2015].
[50] Panagiotakos TB, Fardis MN. Deformations of reinforced concrete members at yielding and ultimate. ACI Struct J 2001;98(2).
[51] Park R, Paulay T. Use of interlocking spirals for transverse reinforcement in bridge columns. Strength and ductility of concrete substructures of bridges, RRU (Road Research Unit). Bulletin 1990;84(1).
[52] Paultre P, Legeron F, Mongeau D. Influence of concrete strength and transverse reinforcement yield strength on behavior of high-strength concrete columns. ACI Struct J 2001;98(4).
[53] Pinheiro J, Bates D. Mixed-effects models in S and S-PLUS. Springer Science & Business Media; 2010.
[54] Pinto PE, Franchin P. Existing buildings: the new italian provisions for probabilistic seismic assessment. In: Ansal A, editor. Perspectives on European earthquake engineering and seismology, number 34 in geotechnical, geological and earthquake engineering. Springer International Publishing; 2014. p. 97–130.
[55] Porter KA, Beck JL, Shaikhutdinov RV. Investigation of sensitivity of building loss estimates to major uncertain variables for the Van Nuys testbed. Technical Report PEER report 2002/03. Berkeley, California: Pacific Earthquake Engineering Research Center, University of California at Berkeley; 2002.
[56] Pujol S. Drift capacity of reinforced concrete columns subjected to displacement reversals [Ph.D. thesis]. Purdue University; 2002.
[57] R Core Team. R: A Language and Environment for Statistical Computing; 2017.
[58] Saatcioglu M, Grira M. Confinement of reinforced concrete columns with welded reinforced grids. ACI Struct J 1999;96(1).
[59] Saatcioglu M, Ozcebe G. Response of reinforced concrete columns to simulated seismic loading. ACI Struct J 1989;86(1).
[60] Sakai Y. Experimental studies on flexural behavior of reinforced concrete columns using high-strength concrete. Trans Jpn Concr Inst 1990;12:323–30.
[61] Scheffe H. The analysis of variance, vol. 72. John Wiley & Sons; 1999.
[62] Searle SR, Casella G, McCulloch CE. Variance components. John Wiley & Sons; 2009.
[63] Sezen H, Moehle JP. Seismic behavior of shear-critical reinforced concrete building columns. In: 7th US national conference on earthquake engineering. Boston: Massachusetts; 2002. p. 21–5.
[64] Soesianawati MT. Limited ductility design of reinforced concrete columns. Technical Report 86-10. New Zealand: University of Canterbury; 1986.
[65] Sugano S. Seismic behavior of reinforced concrete columns which used ultra-high-strength concrete. In: Proceedings of the 11th world conference on earthquake engineering, number 1383. Elsevier Science Ltd.; 1996.
[66] Takemura H, Kawashima K. Effect of loading hysteresis on ductility capacity of reinforced concrete bridge piers. J Struct Eng 1997;43:849–58.
[67] Tanaka H. Effect of lateral confining reinforcement on the ductile behaviour of reinforced concrete columns [Ph.D. thesis]. University of Canterbury, Department of Civil Engineering; 1990.
[68] Thomson JH, Wallace JW. Lateral load behavior of reinforced concrete columns constructed using high-strength materials. ACI Struct J 1994;91(5).
[69] Vamvatsikos D. Seismic performance uncertainty estimation via IDA with progressive accelerogram-wise latin hypercube sampling. J Struct Eng 2014;140:A4014015.
[70] Vamvatsikos D, Cornell CA. Incremental dynamic analysis. Earthquake Eng Struct Dyn 2002;31(3):491–514.
[71] Vamvatsikos D, Fragiadakis M. Incremental dynamic analysis for estimating seismic performance sensitivity and uncertainty. Earthquake Eng Struct Dyn 2010;39(2):141–63.
[72] Watson S. Design of reinforced concrete frames of limited ductility [Ph.D. thesis]. University of Canterbury. Department of Civil Engineering; 1989.
[73] Wehbe NI, Saiidi MS, Sanders DH. Eismic performance of rectangular bridge columns with moderate confinement. ACI Struct J 1999;96(2).
[74] Wight JK, Sozen MA. Shear strength decay in reinforced concrete columns subjected to large deflection reversals. Technical report. University of Illinois Engineering Experiment Station. College of Engineering. University of Illinois at Urbana-Champaign; 1973.
[75] Xiao Y, Martirossyan A. Seismic performance of high-strength concrete columns. J Struct Eng 1998;124(3):241–51.
[76] Xiao Y, Yun HW. Experimental studies on full-scale high-strength concrete columns. ACI Struct J 2002;99(2).
[77] Zahn FA. Design of reinforced concrete bridge columns for strength and ductility [Ph.D. thesis]. University of Canterbury. Department of Civil Engineering; 1985.
[78] Zareian F, Krawinkler H. Assessment of probability of collapse and design for collapse safety. Earthquake Eng Struct Dyn 2007;36(13):1901–14.
[79] Zhou X, Higashi Y, Jiang W, Shimizu Y. Behavior of reinforced concrete column under high axial load. Trans Jpn Concr Inst 1985;7:385–92.
[80] Zhou X, Satoh T, Jiang W, Ono A, Shimizu Y. Behavior of reinforced concrete short column under high axial load. Trans Jpn Concr Inst 1987;9(6):541–8.